

A Preliminary Study of Lower Leg Geometry as a Soft Biometric Trait for Forensic Investigation

Md. Rabiul Islam, Frodo Kin Sun Chan and Adams Wai Kin Kong

School of Computer Engineering

Nanyang Technological University

Singapore

mrabiul@ntu.edu.sg, csfrodochan@ntu.edu.sg and adamskong@ntu.edu.sg

Abstract — Criminal and victim identification is always vital in forensic investigation. Many biometric traits, such as DNA, fingerprint, face and palmprint, have been regularly used by law enforcement agents. However, they are not applicable to legal cases where only non-facial body sites of criminals or victims in evidence images are available for identification. These cases include but not limited to violent protests, masked gunmen and child pornography. To address this challenging identification problem, skin marks, blood vessels hidden in color images, androgenic hair patterns and tattoos have been considered. Tattoos are not always available. Skin marks and blood vessels are suitable for high resolution images. Androgenic hair patterns provide useful identification information even in low resolution images, but their performance is still far from perfect. Thus, new biometric traits are still demanded especially for low resolution evidence images. This paper evaluates lower leg geometry as a soft biometric trait for criminal and victim identification. Lower legs are considered in this study because they are often observable in evidence images. The algorithm utilized in this evaluation first aligns two lower leg shapes from input images and extracts geometric features, including the partial sum of squared difference, the polynomial coefficients and the number of intersection points of the aligned leg shapes. Support vector machines, neural networks and decision trees are used to perform the classification. The algorithm is applied to 1,138 images from 283 subjects. The experimental results indicate that lower leg geometry is an effective soft biometric trait. This study provides a foundation for further research on criminal and victim identification based on body geometry.

Keywords — Forensics, biometrics, skin marks, tattoos

I. INTRODUCTION

Criminal and victim identification is a crucial and challenging task in forensic investigation. Biometric traits, including DNA, fingerprints, palmprints, footprints, shoeprints, signatures, write-prints, face images, face sketches, dental records, have been used regularly by law enforcement agents. All these biometric traits are not applicable to identify criminals and victims in images, where their faces are not observable. Tattoos have been regularly used, but they are not always available. To identify criminals and victims in evidence images of sexual offenses, such as child pornography, skin marks and blood vessel patterns hidden in color images have been proposed recently. These biometric traits are suitable for sexual offenses because evidence images are likely high resolution close-up images [1-2]. For low

resolution evidence images, the challenge still remains because very limited research has been done for it.

Identifying criminals and victims in low resolution images based on non-facial body sites is demanded. In the last several years, because of unstable economic and political environments, many countries experienced violent protests, including Athens riots 2011, London riots 2011, Bahrain riots 2012, Manama riots 2013 and Brazil riot 2013. Violent protestors, who seriously destroy the law and order of many societies, always wear face masks to avoid identification, but it is not uncommon to see their non-facial body sites, in particularly lower legs. Fig. 1 shows six images from London riots 2011, Bahrain riots 2012 and Athens riots 2011. In addition, masked gunmen and terrorists appear in some parts of this world. These cases show clearly that the current biometric traits employed by law enforcement agents are not enough and development of new biometric traits is essential.

To address this challenging identification problem in low resolution images, androgenic hair patterns have been proposed as a biometric trait recently [13]. However, their performance is far from perfect. This paper studies lower leg geometry. Geometric information has been used in commercial biometric systems (e.g., hand geometry [8, 12]) and forensic investigation (e.g., post-mortem identification). Height and weight are also commonly employed as auxiliary information in suspect searches. However, detailed geometric information of body sites is ignored. This paper aims to evaluate this geometric information for criminal and victim identification. Lower legs are selected for this study because they are large and often observable in evidence images. According to our best knowledge, no one performed a similar study before. In this paper, an algorithm with alignment, feature extraction and classification schemes and 1,138 lower leg images from 283 subjects are used in this evaluation.

The rest of this paper is organized as follows: Section 2 presents the testing database. Section 3 explains the algorithm for this evaluation. Section 4 reports the experimental results. Section 5 offers some conclusive remarks.

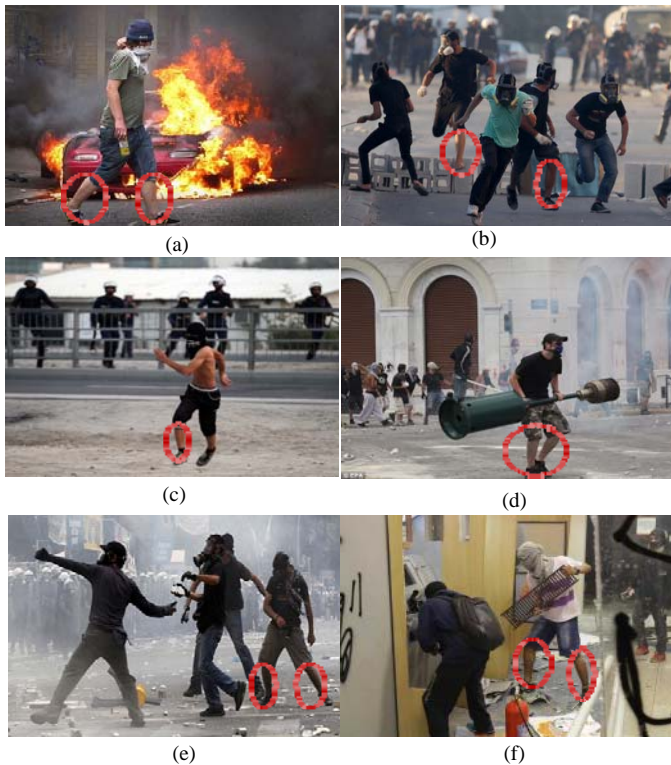


Fig. 1. (a) London riots 2011 [3], (b)-(c) anti-government protesters in Bahrain, Manama [4-5], (d)-(e) Athens riots 2011 [6] and (f) Brazil riot 2013[7].

II. THE TESTING DATABASE

To evaluate lower leg geometry, 1,138 lower leg images from 283 subjects were collected. A Nikon D70s camera and a Canon EOS 500D camera were used in the image collection and their maximum resolutions are respectively $3,008 \times 2,000$ and $4,752 \times 3,168$ pixels. The subjects were mainly Asians, including Chinese, Malays and Indians and all are males. Two sessions of image collection were carried out. In the first session, 575 images were captured and in the second session, 563 images were captured. The average time difference between the two sessions was eleven days. The images collected in the first session were considered as a gallery set, while the images collected in the second session were considered as a probe set in this evaluation. Table 1 summarizes the database. The subjects were not given strict instructions on their poses in the image collection. The lighting environments were changed. Thus, images were collected from viewpoints and illumination conditions. Fig. 2 shows ten unprocessed images (except that they were cropped and resized) in the testing database. Their relative scales are retained. The legs in the testing database were manually cropped and resized to 298 by 142 pixels on average. Fig. 3 shows six pairs of high resolution leg images, where some skin features are highlighted. Their illumination and pose differences are clear. The lower leg shapes of the images are extracted by a semi-automatic approach. First, a method is used to segment the legs and then, their shapes are extracted automatically. If the leg shapes were not segmented correctly, manual correction is carried out. Then, the region of interest defined by six edge points, A, A', M, M', B and B' (Fig. 4(b))

is extracted from the segmented image. MM' is the longest horizontal line within the leg and AA' and BB' are respectively the shortest lines above and below MM. The region of interest is cropped (Fig. 4(c)) and is considered as a preprocessed image for this evaluation. This preprocessing method is modified from Su et al.'s [13]. It should be emphasized that the aim of this paper is neither to develop a new segmentation method for lower leg images nor a complete system for identification. It aims to evaluate the information in lower leg shapes for personal identification. Fig. 5 shows the extracted lower leg shapes for this evaluation.

TABLE I. A SUMMARY OF THE TESTING DATABASE

Number of images	Number of legs collected in the first session	Number of legs collected in the second session
1	5	6
2	265	274
3	12	3
4	1	0

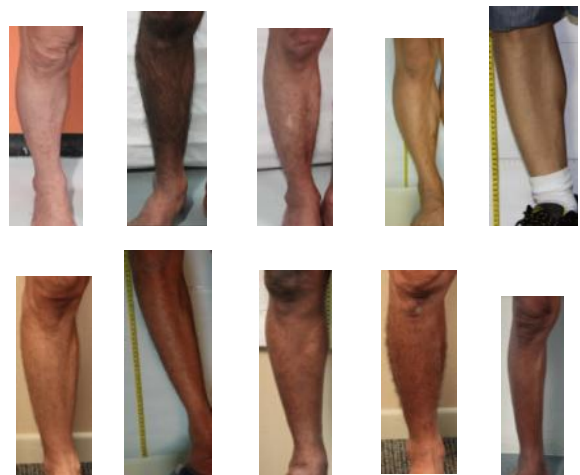


Fig. 2. Ten images in the database.

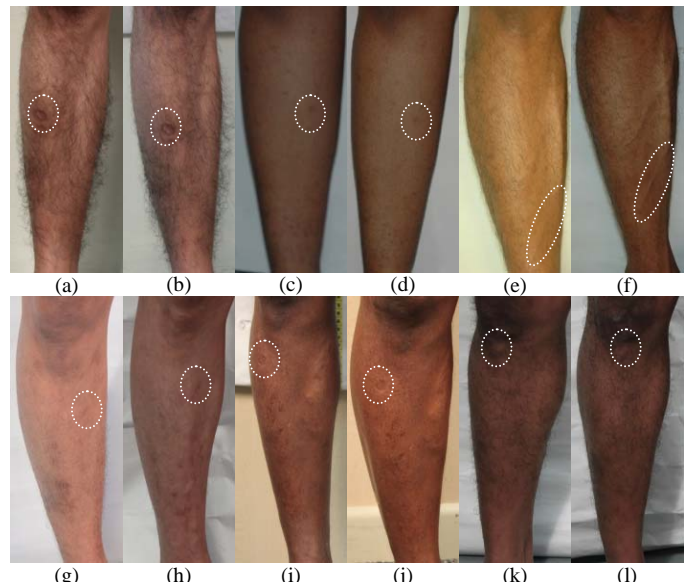


Fig. 3. Images with different pose and illumination from the database

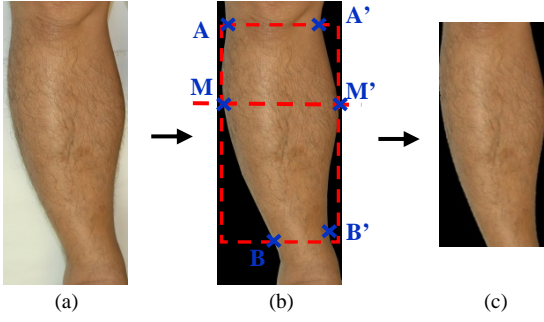


Fig. 4. The preprocessing scheme. (a) An input image. (b) The region of interest is defined by A, A', M, M', B, and B'. The horizontal distance of MM' is the longest and AA' and BB' are the shortest length above and below MM', respectively. (c) The region of interest is extracted as a preprocessed image. Note that AA' and BB' are not necessary to be horizontal lines and the region of interest is the minimum rectangle to include the region between AA' and MM'.

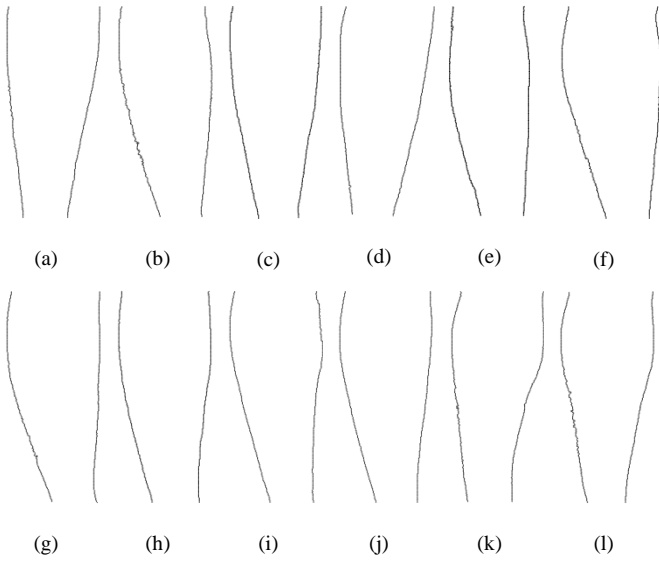


Fig. 5. Examples of lower leg shapes for this evaluation.

III. AN ALGORITHM USED IN THE EVALUATION

In this study, an algorithm with an alignment scheme, a feature extraction scheme and a matching scheme is developed to evaluate geometric information in lower leg shapes. The legs of criminals and victims in evidence images and the legs in a suspect image database (e.g., images collected from ex-prisoners) are collected from different poses and viewpoints and therefore, alignment has to be performed. Figs. 6(a) and (b) show two preprocessed images from the same leg and Fig. 6(c) shows their leg shapes, which are directly overlaid. Figs. 7(a) and (b) show two preprocessed images from different legs and Fig. 7(c) shows their leg shapes, which are directly overlaid. If features are extracted from overlaid shapes without alignment such as Figs. 6(c) and 7(c), the features will be highly influenced by viewpoint and pose variations. In fact, it is very difficult to distinguish whether the shapes in Figs. 6(c) and 7(c) are from the same leg or not. Therefore, alignment is essential before feature extraction.

In order to align the leg shapes, a point set registration method is employed. Point set registration methods assign correspondences between two point sets and determine the transformation between them. There are many point set registration methods for alignment, such as ICP [9], its improved version LM-ICP **Error! Reference source not found.** and the coherent point drift (CPD) [11]. CPD method with an affine transformation is used in this study because it is one of the state of the art methods.

CPD method aligns two point sets through probability density estimation, where one point set is regarded as the centroids of Gaussian Mixture Models (GMM) and the other one is regarded as data points. Then CPD method fits the GMM centroids to the data points by maximizing the likelihood. At the optimum, the point sets become aligned and the correspondences are obtained. The GMM centroids are forced to move coherently as a group to preserve the topological structure of the point sets.

For the sake of clear presentation, a set of notations is given. Given leg shapes from two images, two sets of points in \mathbb{R}^2 are used to represent them. One is denoted as a model set X with size of N_m by 2 and the other is denoted as a data set Y with size of M_d by 2. $T_A(\bullet, \tau_A)$ represents an affine transformation controlled by a parametric vector τ_A . In our alignment scheme, the affine CPD method is used to determine the alignment parameters τ_A . Using the affine transformation parameters τ_A , the point set X is transformed into $X_T = T_A(X, \tau)$. Figs. 6(d) and 7(d) show the alignment results respectively from the leg shapes in Figs. 6 and 7. The shapes from the same leg (Fig. 6(d)) are aligned perfectly, but the shapes from different legs (Fig. 7(d)) still have notable difference.

Because the number of points in X_T and Y may be different, they are sampled to the same size i.e., $X_T = [(x_{ms}(I), y_{ms}(I)), \dots, (x_{ms}(L), y_{ms}(L))]$ and $Y = [(x_{ds}(I), y_{ds}(I)), \dots, (x_{ds}(L), y_{ds}(L))]$, where s represents a sampling function and L represents the total number of sampled points. Let $(x_{mr}(i), y_{mr}(i))$ and $(x_{ml}(i), y_{ml}(i))$ be respectively points on the left and right boundaries in X_T and also let $(x_{dr}(i), y_{dr}(i))$ and $(x_{dl}(i), y_{dl}(i))$ be respectively points on the left and right boundaries in Y . Then, the differences between corresponding points in two aligned boundaries defined

$$A(i) = \sqrt{(x_{mr}(i) - x_{dr}(i))^2 + (y_{mr}(i) - y_{dr}(i))^2} \quad \text{and}$$

$$B(i) = \sqrt{(x_{ml}(i) - x_{dl}(i))^2 + (y_{ml}(i) - y_{dl}(i))^2} \quad \text{are}$$

calculated. The features of the partial sum of squared difference defined below

$$\sum_{i=1}^L A(i), \quad (1)$$

$$\sum_K^{(K+0.1)L} A(i), \quad (2)$$

$$\sum_{i=1}^L B(i), \quad (3)$$

$$\sum_K^{(K+0.1)L} B(i), \quad (4)$$

where $K \in [0.01, 0.1, \dots, 0.9]$, are computed. Eqs. 1-2 and Eqs. 3-4 are the features computed from the aligned right and left boundaries, respectively.

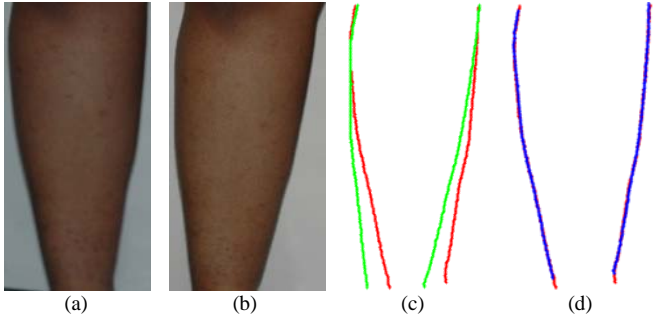


Fig. 6. Alignment of the same leg. (a) – (b) two images of the same leg captured at different sessions. (c) leg shape extracted from (a) and (b) overlaid, and (d) aligned shapes.

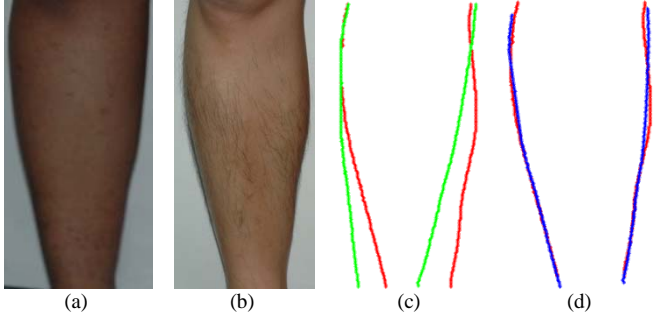


Fig. 7. Alignment of different legs. (a) – (b) images of different legs, (c) leg shapes extracted from (a) and (b) overlaid, and (d) aligned shapes.

In addition to the partial sum of squared difference, polynomial coefficients derived from the two sequences $A(i)$ and $B(i)$ are also used as features. Since the leg shapes are aligned, the polynomial coefficients can be directly computed. Two second-order polynomials, $f_A(x) = a_2x^2 + a_1x + a_0$ and $f_B(x) = b_2x^2 + b_1x + b_0$, where a_0, a_1, a_2, b_0, b_1 and b_2 are the polynomial coefficients, are fitted on $A(i)$ and $B(i)$, respectively. The normalized coefficients $a_j/\max(a_k)$ and $b_j/\max(b_k)$, where j and $k \in \{0,1,2\}$, are used as features. Furthermore, the numbers of intersection points of two aligned shapes are also included as features. Figs. 8(a) and 8(b) depict the intersection points of the same leg and different legs respectively.

In total 30 features, including 11 partial sums from aligned left boundaries (Eqs. 1-2), 11 partial sums from aligned right boundaries (Eqs. 3-4), 2 numbers of intersection points and 6 polynomial coefficients are obtained from two aligned shapes. The first 24 features are normalized to zero and one through a training database and the rest are used directly. Feature selection based on the mutual information proposed by Peng et al. [14] is performed. Three classification methods, support vector machines (SVM), neural network (NN) and decision tree (DT) are employed to validate the selected features and for the final evaluation.

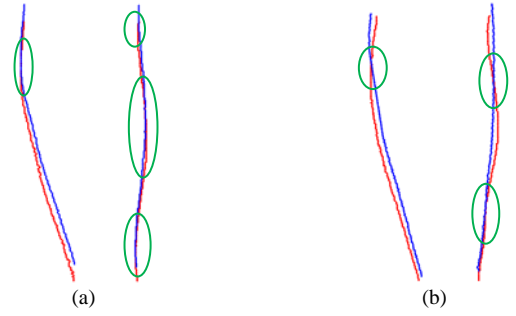


Fig. 8. Intersection points on the aligned leg shapes and (a) shapes from the same leg and (b) shapes from different legs.

IV. EXPERIMENTAL RESULTS

The lower leg shapes in the probe set were matched with those in the gallery set. A dataset of 1,138 images from 283 legs was collected. There were 575 images in the probe set and 563 images in the gallery set. Each leg shape was sampled to 256 points. To each pair of images, one from the probe set and the other from the gallery set, we applied the algorithm elaborated in Section III and obtained 323,725 (563×575) feature vectors. For the sake of training, 2-fold cross validation was applied to the probe set and the gallery set. In the first fold, 287 images in the probe set and 283 images in the gallery set were used for training; the rest were used for testing. In the second fold, the same 287 images in the probe set and the same 283 images in the gallery set were used for testing; the rest were used for training.

For SVM, a radial basis function was used as a kernel and the gamma value was set to 0.07. For NN, a feedforward network was used and the number of hidden neurons was ten. For DT, default parameters in Matlab were used, except for the parameter, minleaf, which was set to 30. Because the positive (genuine) and negative (imposter) training data are very imbalanced, sampling was performed. In the first (second) fold, we selected 574 (571) genuine feature vectors from the 287 (288) images as positive training data and randomly selected 574 (571) imposter feature vectors as negative training data. Note that most of the legs have four images in our database and therefore we can have more than 500 genuine feature vectors in one fold. The training data was further split into two parts. One is for selecting features and the other is for validating the selected features. 10 fold-cross validation was used in this feature selection process. Table II summarizes the selected features for different classifiers. All most all the polynomial coefficients and the numbers of intersection points were selected. The entire training set and the selected features were used to train the classifiers for final evaluation.

TABLE II. A SUMMARY OF THE SELECTED FEATURES

	SVM		NN		DT	
	fold 1	fold 2	fold 1	fold 2	fold 1	fold 2
Training data	fold 1	fold 2	fold 1	fold 2	fold 1	fold 2
Partial sum of squared difference Eq. 1-Eq.4 (total 22)	20	22	16	16	15	12
Polynomial coefficients (Total 6)	6	6	6	6	6	5
Number of intersection points (Total 2)	2	2	2	2	2	2

The trained classifiers were applied to the testing data. Each classifier gives a similarity value to each testing datum and it is used to plot cumulative match characteristic (CMC) curves given in Fig. 9. The corresponding rank-1, rank-10 and rank-20 accuracies are given in Table III. The rank-1 accuracies given by SVM and NN are over 40% and their rank-20 accuracies are over 80%. Although the testing databases in the two folds were formed by around 140 different legs, this performance is out of our expectation because we feel that leg shapes of different persons are similar. The experimental results indicate clearly that lower leg geometry is an effective soft biometric trait.

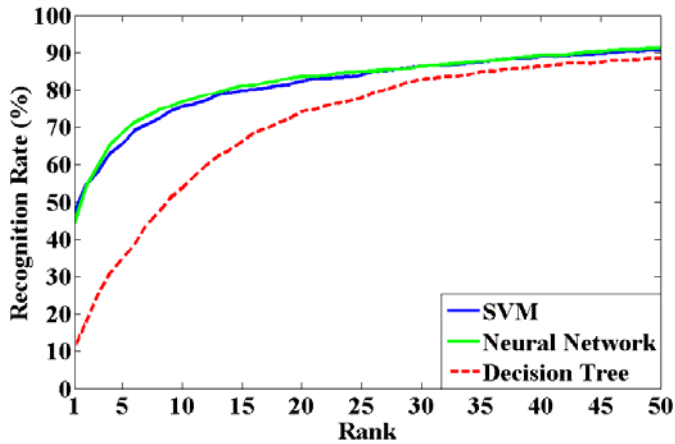


Fig. 9 Cumulative match characteristic curves

TABLE III. A SUMMARY OF THE EXPERIMENTAL RESULTS

Classifier	Rank-one accuracy	Rank-10 accuracy	Rank-20 accuracy
SVM	47.13%	75.65%	82.26%
NN	44.52%	74.96%	82.61%
DT	3.83%	33.22%	65.04%

V. CONCLUSION

Identifying masked criminals in digital images is a challenging task. Even though tattoos, skin marks, androgenic hair patterns and blood vessels hidden in color images have been considered, they have different weaknesses. Tattoos are not always available. Skin marks and blood vessels require high resolution images. Androgenic hair patterns are suitable for low resolution images. However, their performance is still far from perfect. Currently, forensic agents use a number of soft biometric traits, e.g., height, weight, races and genders in investigation. However, body shape is ignored. Lower legs are selected for this study because they are often observable in evidence images (e.g., violent protesters). A feature set comprised of the partial sum, the polynomial coefficients and the number of intersection points of aligned leg shapes and three classification methods are used in this evaluation. The experimental results indicate that lower leg shapes contain quality information as a soft biometric trait. These results encourage further study on lower legs and full body geometry for forensic investigation.

ACKNOWLEDGMENT

We would like to thank the U.S. Department of Justice, the U.S. Immigration and Customs Enforcement, the Singapore Prison Service, and the Singapore Police Force for providing legal and forensics information. This work is partially supported by the Ministry of Education, Singapore through Academic Research Fund Tier 2 MOE2012-T2-1-024.

REFERENCES

- [1] A. Nurhudatiana, A.W.K. Kong, K. Matinpour, D. Chon, L. Altieri, S. Y. Cho and N. Craft, "The individuality of relatively permanent pigmented or vascular skin marks (RPPVSM) in independently and uniformly distributed patterns", *IEEE Transactions on Information Forensics and Security*, vol. 8, no. 6, pp. 998-1012, 2013.
- [2] C. Tang, A.W.K. Kong and N. Craft, "Uncovering vein patterns from color skin images for forensic analysis", *Proc. of IEEE Computer Vision and Pattern Recognition*, pp. 665-672, 2011.
- [3] "London riots spread as police lose control", *The Age* Aug. 9, 2011 [Online]. Available: <http://www.theage.com.au/world/london-riots-spread-as-police-lose-control-20110809-1ijmm.html>
- [4] "Bahrain clears 21 medics of protest charges", *Yahoo News* Mar. 28, 2013 [Online]. Available: <http://news.yahoo.com/bahrain-clears-21-medics-protest-charges-104533403.html>
- [5] "Bahrain Air grounded by mounting debts", *Yahoo News* Feb. 13, 2013 [Online]. Available: <http://news.yahoo.com/bahrain-air-grounded-mounting-debts-073854094--finance.html>
- [6] "The £25bn bombshell: rioters stone MP after Greece pushes through austerity package", *Daily Mail* June 30, 2011 [Online]. Available: <http://www.dailymail.co.uk/news/article-2009437/Greek-vote-Rioters-stone-MP-Greece-pushes-austerity-package.html>
- [7] "Huge protests continue in Brazil — small bands of radicals break into stores and loot", *Business Insider* Jun. 19, 2013 [Online]. Available: <http://www.businessinsider.com/huge-protests-continue-in-brazil-small-bands-of-radicals-break-into-stores-and-loot-2013-6>
- [8] R. Sanchez-Reillo, C. Sanchez-Avila and A. Gonzalez-Marcos, "Biometric identification through hand geometry measurements", *IEEE Transactions on Pattern Analysis and Machine Intelligence*, vol. 22, no. 10, pp. 1168-1171, 2000.
- [9] P. Besl and N. McKay, "A method for registration of 3-D shapes", *IEEE Transactions on Pattern Analysis and Machine Intelligence*, vol. 14, no. 2, pp. 239-256, 1992.
- [10] A. Fitzgibbon, "Robust registration of 2D and 3D point sets", *Image and Vision Computing*, vol. 21, no. 13-14, pp. 1145-1153, 2003.
- [11] A. Myronenko and X. Song, "Point set registration: coherent point drift", *IEEE Transactions on Pattern Analysis and Machine Intelligence*, vol. 32, no. 12, pp. 2262-2275, 2010.
- [12] C. Oden, A. Ercil, and B. Buke, "Combining implicit polynomials and geometric features for hand recognition," *Pattern Recognition Letters*, vol. 25, no. 13, pp. 2145-2152, 2003.
- [13] H. Su and A.W.K. Kong, "An evaluation on low resolution androgenic hair patterns for criminal and victim identification," *IEEE Transactions on Information Forensics and Security*, conditionally accepted.
- [14] H. Peng, F. Long, and C. Ding, "Feature selection based on mutual information: criteria of max-dependency, max-relevance, and min-redundancy," *IEEE Transactions on Pattern Analysis and Machine Intelligence*, vol. 27, no. 8, pp.1226-1238, 2005.